J Mater Sci (2006) 41:7590–7596
DOI 10.1007/s10853-006-0847-4

A study on the diffusion kinetics of borides on boronized Cr-based steels

Sukru Taktak

Received: 18 August 2005 / Accepted: 11 November 2005 / Published online: 15 September 2006

Abstract In the present study, kinetics of borides formed on AISI H13 hot work tool and AISI 304 stainless steels have been investigated. Boronizing treatment was carried out in slurry salt bath consisting of borax, boric acid and ferrosilicon at temperature range of 1073–1223 K for 3, 5 and 7 h. X-ray diffraction analysis of boride layers on the surface of steels revealed various peaks of FeB, Fe_2B, CrB and Ni_3B. Metallographic studies revealed that the boride layer has a flat and smooth morphology in the 304 steel while H13 steel was a ragged morphology. Depending on temperature and layer thickness, the activation energies of boron in 304 and H13 steels were found to be 253.35 and 244.37 kJ mol^{-1}, respectively.

Introduction

One of the surface treatments is boronizing which is technically well developed and widely used in industry to produce extremely hard and wear resistant surface layer on metallic substrate. Diffusion boronizing is a thermo-chemical treatment that permits boride layers of good performance properties to be produced on steels. The boronized steels exhibit high hardness (about 2000 HV), high wear resistance and improved corrosion resistance [1–4]. Boron atoms can diffuse into ferrous alloys due to their relatively small size and very mobile nature. They can dissolve in iron interstitially, but can react with it to form FeB and Fe_2B intermetalic compounds. Depending on the potential of medium and chemical composition of base materials, single or duplex layer may be formed. During boronizing of ferrous alloys, generally, a boron-compound layer develops which consists of a surface-adjacent FeB sublayer on top of a Fe_2B sublayer [5, 6]. Boronizing can be applied to a wide range of steel alloys including carbon steel, low alloy-steel, tool steel and stainless-steel. In addition, materials such as nickel based alloys, cobalt based alloys, tungsten and niobium can be boronized to obtain very high hardness and wear resistance on their surfaces [7–10].

To control the boronizing processes, knowledge of kinetic parameters is essential. Some kinetics models have been developed for the establishment of the variables that affect the boronizing process. It is very important to establish the variables that affect the boronizing kinetics process to control automated procedures and obtain desirable properties [11].

Austenitic stainless steels and hot work tool steels have high chromium content and are commonly used engineering materials. These are also well-suited and established for surface treatments such as nitriding and boronizing. Most studies about boronizing of steels and non-ferrous metals have done. However, a little knowledge about examination of growth kinetics of borides formed on boronized AISI H13 and AISI 304 in borax based salt bath. In this study, the boron diffusion on boride layer is evaluated by taking into account experimental data for growth kinetics of the boride layers during the molten salt bath boronizing process on AISI H13 and 304 steels. The growth kinetics of the layer is analyzed by measuring the

S. Taktak (✉)
Technical Education Faculty, Department of Metal Education, Afyon Kocatepe University, Afyon, Turkey
e-mail: taktak@aku.edu.tr

thickness of the layer as a function of the boriding time within a temperature range of 1073–1223 K.

Experimental procedures

Substrate materials and boronizing

AISI H13 hot work tool steel and AISI 304 stainless steel were used in this work. Both steels have a very widespread use in the industry and improvement of their surface properties are especially important for both corrosion resistance and load bearing. The chemical compositions are given in Table 1. The test samples have dimensions of ∅20 × 6 mm. Before boronizing treatment, the specimens were ground up to 1200 mesh emery paper and polished. Boronizing was carried out using the slurry salt bath consisting of borax (60 wt.%) and boric acid (20 wt.%) as a boron source and ferro-silicon (20 wt.%) as the activator. Boronizing treatments were performed in an electrical resistance furnace at temperature of 1073–1223 K at 50 K intervals for holding time of 3, 5 and 7 h. Selected boronizing temperatures, durations and medium contents are in agreement with the literatures [1, 12]. Test materials to be boronized were immersed in a slurry salt bath using a sealed container. Having completed the boronizing heat treatment, test samples were removed from the bath and quenched in air.

Characterization of the boride layers

For the characterisation purpose scanning electron microscopy (SEM), energy dispersive X-ray spectroscopy (EDX) and X-ray diffraction (XRD) analysis are carried out. The microstructures of polished and etched cross-sections of the specimens were observed by a Leo 1430 VP scanning electron microscope. The nature and type of borides formed in coating layer are closely related to chemical composition of substrates concerned. The presence of borides formed in the coating layer was confirmed by means of X-ray diffraction (Shimadzu XRD 6000) using Cu K_α radiation. The thicknesses of borides were measured by means of a digital thickness measuring instrument attached to an optical microscope (Olympus BX60). Thickness values are averages of at least 12 measurements. The hardness of the borided steel materials was also measured using a digital microhardness tester fitted with a Vickers indenter under loads of 100 g.

Table 1 Chemical composition of test materials

Steel	Chemical composition, % by weight								
	C	Cr	Ni	Si	Mn	Mo	V	S	P
AISI H13	0.4	5.3	–	1	0.3	1.4	1	0.005	0.025
AISI 304	0.04	18.3	8.7	1	2	–	–	0.03	0.045

Results

Microstructure and characterization

Figures 1 and 2 show SEM view of AISI H13 and 304 steels boronized at 1123 and 1223 K for 5 h. As can be seen the borides formed on the stainless steel substrate have a smooth and flat morphology when compared to borides formed on the surface of hot work tool steel. These figures revealed that the boride layers increased with increasing treatment temperature. The XRD patterns of the boronized steels at 1173 K for 5 h are given in Fig. 3. The presence of phases of boride layers

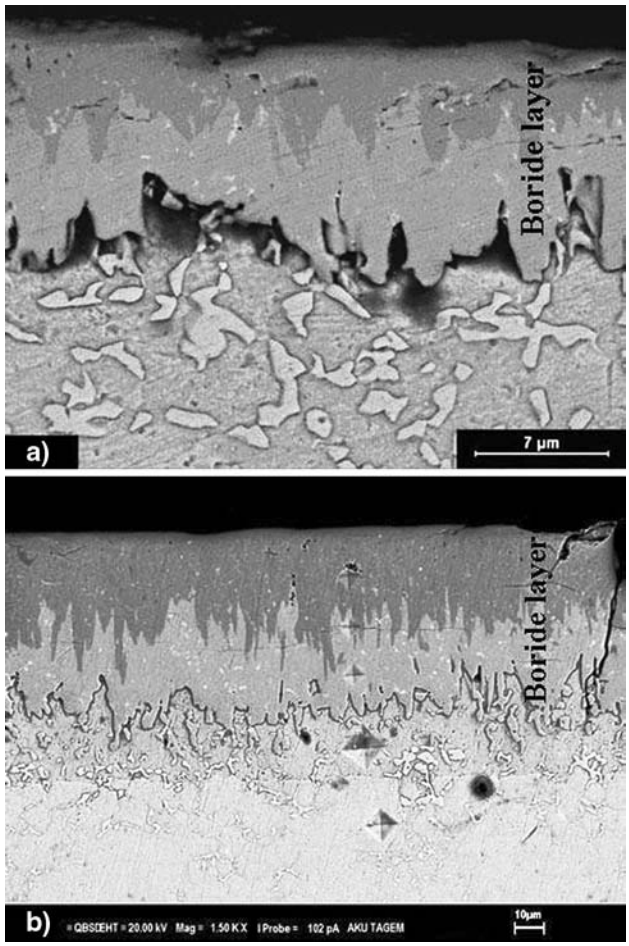

Fig. 1 SEM-BE Image of microstructure of AISI H13 hot work tool steel boronized at; (**a**) 1123 K and (**b**) 1223 K for 5 h

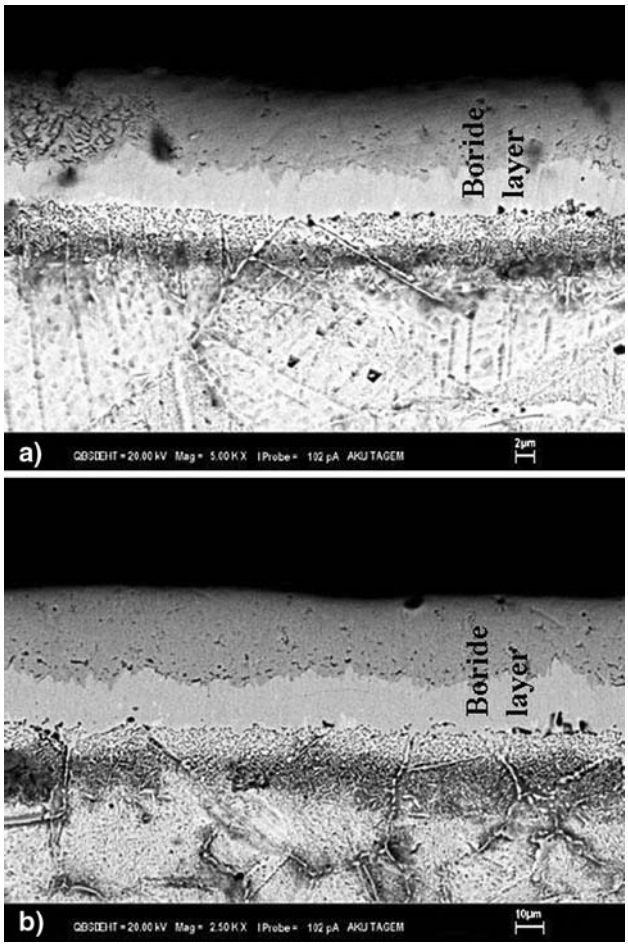

Fig. 2 SEM-BE Image of microstructure of AISI 304 austenitic stainless steel boronized at; (**a**) 1123 K and (**b**) 1223 K for 5 h

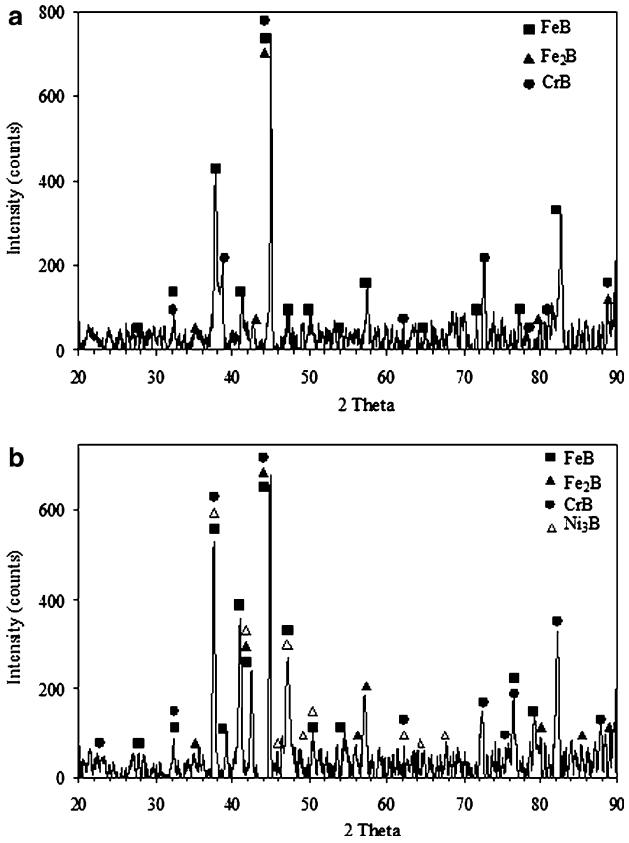

Fig. 3 XRD pattern of (**a**) AISI H13 and (**b**) AISI 304 steels boronized at 1173 K for 5 h

for tool steel and stainless steel are Fe_2B, FeB, CrB and FeB, Fe_2B, CrB, Ni_3B respectively. The hardness values of unboronized and boride layer formed on boronized steels are given in Table 2. The hardness values of boride layers are much higher than that of substrates.

Layer growth and kinetics

Figures 4 and 5 shows SEM micrographs and EDX spectrums of the illustrated points with A, B, C and D letters for both steels boronized at temperature of 1123 K for 5 h duration. As it can be seen in Fig. 4b, Cr and Fe elements concentrate in the coating layer to form FeB, Fe_2B and CrB phases. V and Mo elements are observed in the boride coating layer. But the boride phases of these elements are not seen in the XRD pattern. EDX analysis carried out on the boronized 304 stainless steel (Fig. 5b) indicates that Cr, Fe and Ni elements concentrate in the coating layer to form borides of Fe, Cr and Ni. At the interface, concentration of Ni is higher than that of both boride layer and base metal. This case can be attributed to the formation of Ni-rich zone underneath the boride layers. Furthermore silicon concentrates strongly at the interface for both steels as it is insoluble in iron borides.

Figure 6 shows the influence of boronizing time and temperature in the layer's depth. In addition, Fig. 6 represents an apparent linear relation between the thickness of the boride layers of both steels and $\sqrt{t}$. This suggests a simple diffusion-controlled growth behaviour. The thicknesses of boride layers are in the range of 8–58 μm for H13 and 4–42 μm for 304 steels, depending on the boriding time and temperature. Furthermore, contour diagrams derived from Fig. 6 by means of Sigma plot 7.0 software. This allows that the selection of process parameters such as time and

Table 2 Hardness values for substrate and boride layers

Steel	Substrate hardness ($HV_{0.1}$)	Average boride layer hardness ($HV_{0.1}$)
AISI H13	430	1860
AISI 304	205	2150

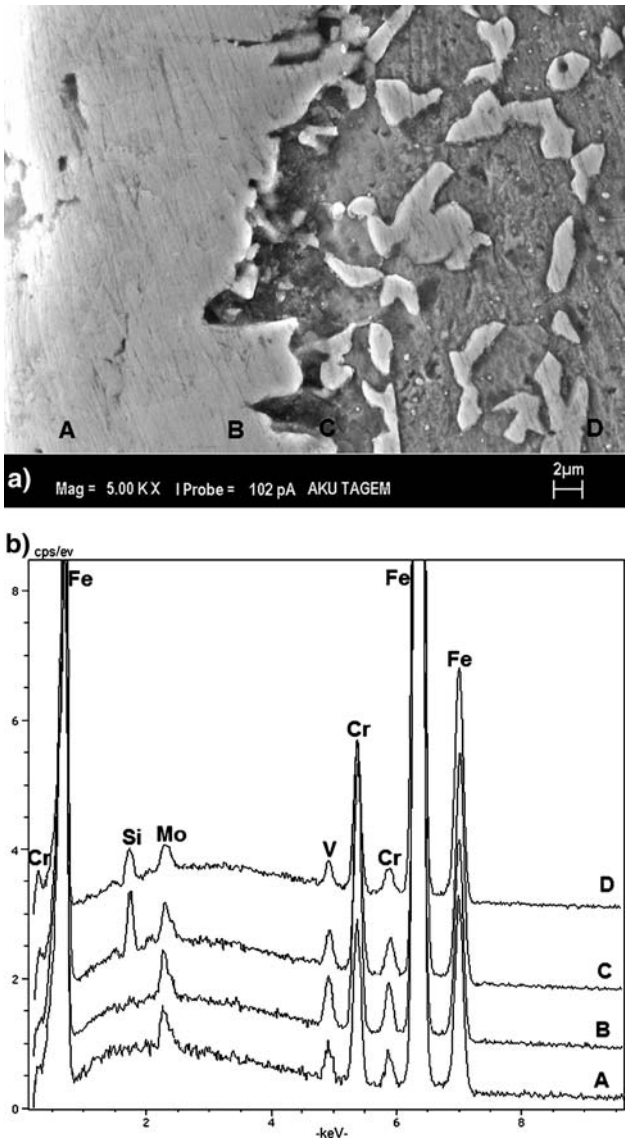

Fig. 4 (**a**) SEM micrograph of AISI H13 tool steel boronized at 1123 K for 5 h, (**b**) EDX spectrums of the illustrated points with A, B, C and D letters

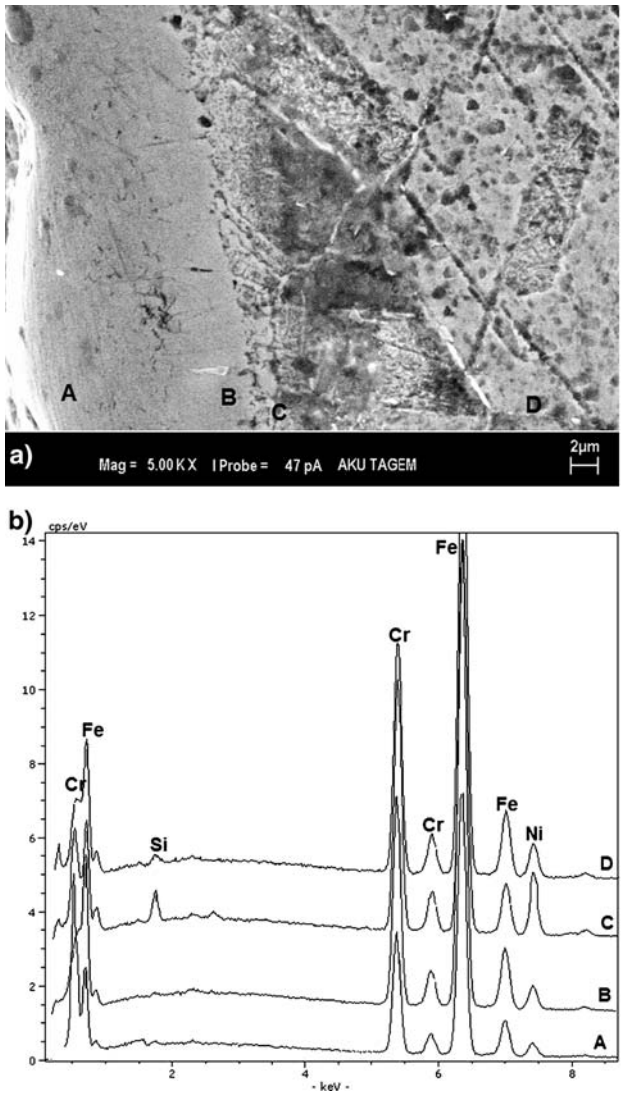

Fig. 5 SEM micrograph of AISI 304 stainless steel boronized at 1123 K for 5 h and EDX spectrums of the illustrated points with A, B and C letters

temperature for obtaining a predetermined coating layer thickness in industrial application (Fig. 7). Empirical equations for boride layer thickness on the steels of H13 and 304 are constructed with the correlation coefficient (R^2) of 0.9958 and 0.996 as follows:

$$x_{\mathrm{H13}} = 132\ \mathrm{e}^{-0.5\left[\left(\frac{T-1399}{148.4}\right)^2+\left(\frac{t-10.6}{8.4}\right)^2\right]} \quad (1)$$

$$x_{304} = 185\ \mathrm{e}^{-0.5\left[\left(\frac{T-1285}{110.3}\right)^2+\left(\frac{t-32.8}{15.75}\right)^2\right]} \quad (2)$$

where x is the layer thickness (μm); T is the boriding temperature (K) and t is time (h).

The thickness of the boride layer as a function of squared time is described by:

$$x = K \cdot \sqrt{t} \quad (3)$$

where K is the growth rate constant depending on the diffusion element and diffusion coefficient. Generally, it is expected that the plot of boride layer thickness versus squared treatment time gives a straight line which indicates the growth of layer has a parabolic dependence to time. The values of K were calculated from the slopes of the layer thickness versus squared treatment time graphs (Fig. 6). The relationship between growth rate constant and temperature can be expressed by an Arrhenius type equation as:

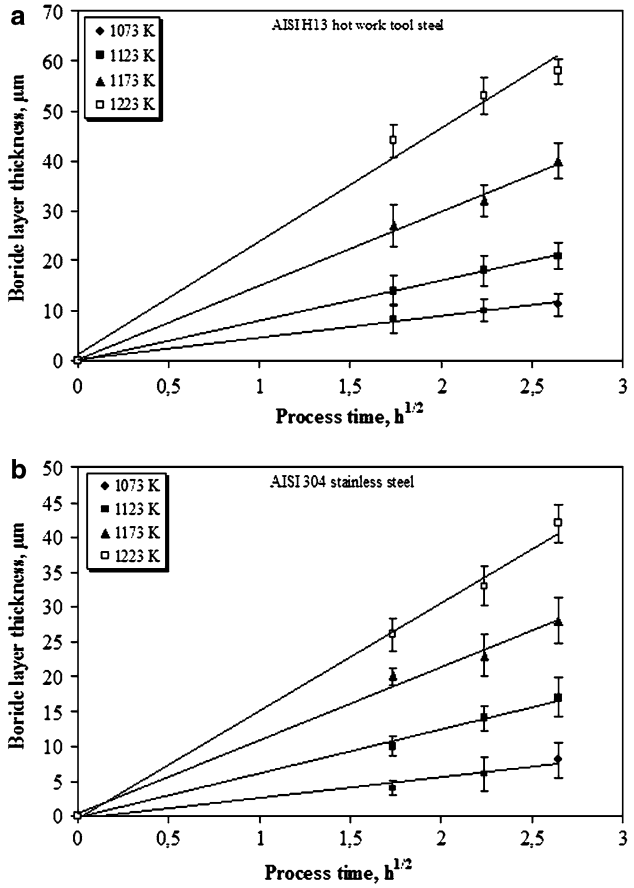

Fig. 6 Boride layer thickness versus boronizing time at various temperatures for: (**a**) AISI H13 steel and (**b**) AISI 304 steel

$$K = K_0 \exp\left(-\frac{Q}{R \cdot T}\right) \tag{4}$$

where Q is the activation energy (kJ mol^{-1}); T is the absolute temperature (K) and R is the gas constant (kJ mol^{-1} K^{-1}). Figure 8 is the plot of growth rate constant of the boride layer of H13 tool and 304 stainless steels as a function of temperature. Consequently, the activation energy for the boron diffusion in the boride layer is determined by the slope obtained by the plot of ln$K$ vs. $1/T$. Making use of the least-squares analysis, the kinetics conclusions are obtained as:

$$K_{\mathrm{H13}} = 44.03 \exp\left(-\frac{244.37}{R \cdot T}\right) \tag{5}$$

$$K_{304} = 51.9 \exp\left(-\frac{253.35}{R \cdot T}\right) \tag{6}$$

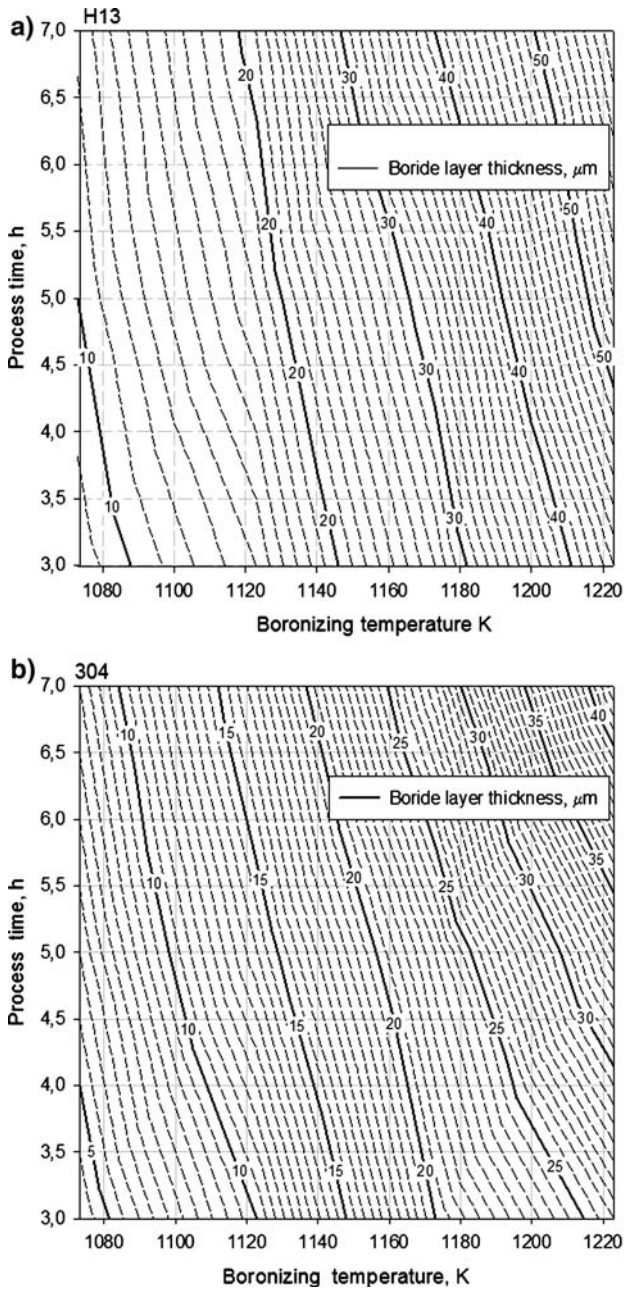

Fig. 7 Contour diagram of boride layer thickness of boronized: (**a**) AISI H13 steel and (**b**) AISI 304 steel

for the temperature range of 1073 K to 1223 K. In addition, growth rate constant K and activation energy Q values are listed in Table 3.

Discussion

SEM-BEI cross-sectional observation of borides formed on the surface of H13 steel show a saw-tooth morphology. However, saw-tooth nature tendency of

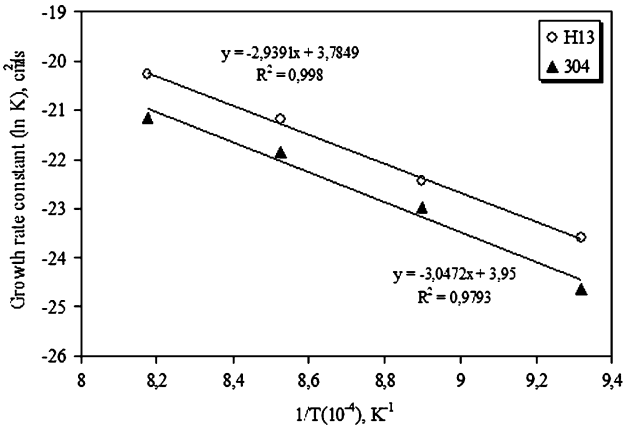

Fig. 8 Growth rate constant versus temperature of boronized AISI H13 tool steel and AISI 304 stainless steel

boride layer was less when compared to borides formed on the surface of plain carbon steel [12]. The flat boride morphology appeared on the surface of the 304 stainless steel, since the diffusion was more restricted due to the presence of a high content of alloying elements (Cr, Ni). When the chromium content of steel is increased, boride layer formed on the steel would be thinner and interface between boride layer and matrix takes smooth morphology [13]. Microstructure and mechanical properties of boronized hot work tool steel and stainless steel depended strongly on chemical composition, process temperature and boronizing time. It is observed that coating layer formed on the hot work tool and the stainless steels substrate essentially have three distinct regions which are; (i) layers having borides (i.e. FeB, Fe_2B, CrB and FeB, Fe_2B, CrB, Ni_3B respectively), (ii) the region below boride layers, where boron makes solid solution, which has hardness less than that of borides, and (iii) steel matrix, which is not affected by boron.

Previous studies showed that boronizing of carbon steels usually leads to formation of two borides, FeB and Fe_2B, where FeB was located near the surface and Fe_2B in the vicinity of steel matrix [12, 14]. In the present study, the presence of borides was identified via XRD analysis (see Fig. 3). XRD results show that boride layers formed on the hot work tool and stainless steels contain Fe_2B, FeB, CrB and FeB, Fe_2B, CrB, Ni_3B phases respectively. The tool steel contains the Mo (1.4 wt.%) and V (1 wt.%) elements. The enthalpies of formation of vanadium borides are negatively much higher than the enthalpies of formation of chromium borides and iron borides [15]. Therefore, it is highly probable that vanadium and molybdenum borides are formed in the boride layer. However the borides of these elements are not seen in the XRD pattern. EDX analysis shows that Fe, Cr and Fe, Cr, Ni concentrated in the coating layers formed on the surfaces of H13 tool and 304 stainless steels, respectively. It can be observed that Ni-rich layer takes place underneath the boride layer on the stainless steel as previously observed by other researchers [16, 17]. Silicon, which was insoluble in iron borides, concentrates strongly at the interface for both steels.

The layer growth for both steels show that the layer thickness changes parabolically with time. It can be observed that the boride layer thickness reduces with increasing the amount of alloying element. The coating thickness is influenced by alloying elements in the metal substrate (especially by chromium), which can modify the active boron diffusivity by entering the iron boride lattice [18]. In addition, Carbucicchio et al. [19] reported that with increasing contents of the third alloying element in the alloys, both the depth of FeB-base region and the FeB/FeB_x ratio increases in the case of chromium-containing alloys. Chromium tends to concentrate within the coating layers.

The growth rate of boride layer is controlled by boron diffusion in the FeB and Fe_2B sublayers and boride layer growth occurs as a consequence of boron diffusion perpendicular to the surface of the specimen. The calculated values of activation energies for the boronizing process in the H13 and 304 steels are about 244.37 and 253.35 kJ mol^{-1}, respectively. The activation energies of boronized H13 and 304 steels are different. It is well known that this difference in the activation energies caused from high Cr and Ni contents of 304 steel. The kinetics results of the present study are effectively comparable with Refs. [5, 16, 20–23] as seen in Table 4. Especially, Ref. [16] studied the same steel (AISI 304) with different boronizing

Table 3 Growth rate constant (K) and activation energy (Q) as a function of boronizing temperature and steel

Steel	Growth rate constant ($cm^2\ s^{-1}$)				Activation energy (kJ mol^{-1})
	Temperature, K				
	1073	1123	1173	1223	
AISI H13	5.64×10^{-11}	1.79×10^{-10}	6.26×10^{-10}	1.56×10^{-9}	244.37
AISI 304	2×10^{-11}	1.05×10^{-10}	3.25×10^{-10}	6.44×10^{-10}	253.35

Table 4 The comparison of activation energy for diffusion of boron with respect to the different boronizing medium and steel

Steel	Temperature range (K)	Boronizing medium	Activation energy (kJ mol^{-1})	References
AISI W1	1123–1323	Salt bath	171.2	20
AISI 5140, 4340, D2	1123–1223	Salt bath	223, 234, 170	21
Fe–Cr–Ni	1025–1275	Pack	156	5
AISI 1045	1193–1273	Paste	226.7	22
AISI 304	1023–1223	Plasma paste	123	16
Pure iron	1223–1323	Paste	151	23
AISI H13, 304	1073–1223	Salt bath	244.37, 253.35	Present study

medium. Present study gives the highest activation energy. This case suggests that activation energy varies with the boron potential of the medium. We believe that the alloying elements, e.g. Cr and Ni, of boronized steels affected the results. It can be considered that alloying elements acted as a diffusion barrier, inhibiting the diffusion of active boron.

Conclusions

In this study, we investigated some properties of borides on the surface of boronized AISI H13 hot work tool and AISI 304 stainless steels. Following conclusions can be drawn from the results.

- Non-oxide ceramic boride types formed on the surface of the H13 steel had a saw tooth morphology. Whereas, the flat and smooth morphology appeared on the boride layer of the 304 stainless steel.
- The polyphase boride coatings thermochemically grown on H13 and 304 steels were constituted by FeB, Fe_2B, CrB and FeB, Fe_2B, CrB, Ni_3B phases, respectively. Ni-rich zone formed underneath the boride layer on the 304 steel. However, silicon concentrated strongly at the interface of coating and substrate.
- The boride layer thickness changed parabolically with time for both steels and it reduced with increasing the amount of alloying element (especially chromium). An empirical equation was suggested for estimating the layer thickness as a function of process time and temperature. The activation energies for the formation of the boride layer in H13 and 304 steels were found to be 244.37 and 253.35 kJ mol^{-1}, respectively. H13 steel had lower activation energy when compared to that of 304 steel due to probably low alloying element, acting as a diffusion barrier.

References

1. Sinha AK (1991) Boronizing, vol 4. ASM International Heat Treating, Cleveland, p. 437
2. Carbucicchio M, Palombarini GP (1987) J Mater Sci Lett 6:1147
3. Mann BS (1997) Wear 208:125
4. Hu R, Fenske GR, Rehn LE, Baldo PM, Erdemir A, Lee RH, Erck RA (1990) Surf Coat Technol 42(3):283
5. Brakman CM, Gommers AWJ, Mittemeijer EJ (1989) J Mater Res 4(6):1354
6. Singhal SC (1977) Thin Solid Films 45(2):321
7. Usta M (2005) Surf Coat Technol 194:251
8. Jain V, Sundararajan G (2002) Surf Coat Technol 149:21
9. Usta M, Ozbek I, Ipek M, Bindal C, Ucisik AH (2005) Surf Coat Technol 194:330
10. Ueda N, Mizukoshi T, Demizu K, Sone T, Ikenaga A, Kawamoto M (2000) Surf Coat Technol 126:25
11. Melendez E, Compas I, Rocha E, Barron MA (1997) Mater Sci Eng A234:900
12. Bindal C, Ucisik AH (1999) Surf Coat Technol 122:208
13. Hunger HJ, True G (1994) Heat Treat Met 2:31
14. Pelleg J, Judelewics M (1992) Thin Solid Films 215(1):35
15. Barin I, Knacke O (1973) Thermochemical properties of inorganic substance. Springer-Verlag, Berlin, p 830
16. Yoon JH, Jee YK, Lee SY (1999) Surf Coat Technol 112:71
17. Ozbek I, Konduk BA, Bindal C, Ucisik AH (2002) Vacuum 65:521
18. Pertek A, Kukla M (2002) Appl Surf Sci 202:252
19. Carbucicchio M, Palombarini G, Sambogna G (1984) J Mater Sci 19(12):4035
20. Genel K, Ozbek I, Bindal C (2003) Mater Sci Eng A347:311
21. Sen S, Sen U, Bindal C (2005) Surf Coat Technol 191:274
22. Campos I, Bautista O, Ramirez G, Islas M, De La Parra J, Zuniga L (2005) Appl Surf Sci 243:429
23. Campos I, Oseguera J, Figureoa U, Garcia JA, Bautista O, Kelemenis G (2003) Mater Sci Eng A352:261